

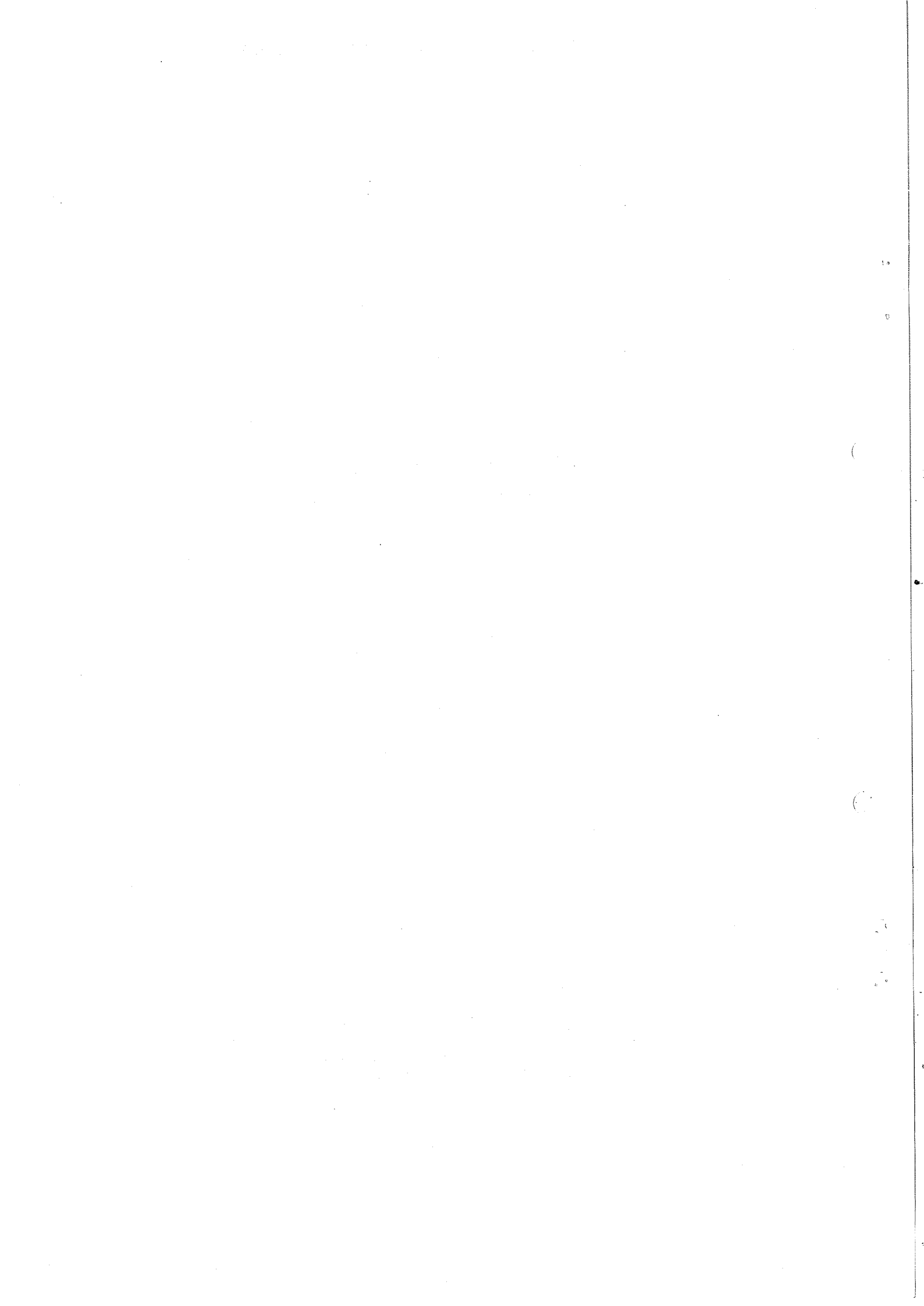
ON VACUUM POLARIZATION IN MUONIC ATOMS
AND SOME RELATED TOPICS

E. Zavattini

CERN, Geneva, Switzerland

Lecture to be given at the
"Ettore Majorana" Centre for Scientific Culture;
Exotic atoms and related topics.
Erice, Sicily, 24-30 April 1977.

Geneva - 25 March 1977



1. INTRODUCTION

All observed phenomena due to the interaction of the electromagnetic field and the electron (muon) field -- at least up to momentum transfer to the electrons or photons of a few GeV/c -- can be quantitatively described by the present QED theory: this is true up to the precision with which today we can perform measurements on "test" experiments.

As usual also in QED, a particular physical situation of photons and electrons is described by a suitably definite state vector: it is one of the most important assumptions of QED, the existence of a *physical state* which is a state of minimum energy called "the vacuum state".

Among the typical predictions of QED which mostly bring out the difference with the classical theory of electron and photon, are those facts connected with the presence of such a vacuum state. We recall

- i) the vacuum fluctuations of the electromagnetic field: typical effects are the spontaneous emission, the "Lamb shift", etc.;
- ii) the electronic vacuum polarization: typical effects of this phenomenon are the modification of the Coulomb law in the vicinity of a charge, non-linear effect in electromagnetic phenomena (photon-photon interaction), etc.

After a brief historical introduction, these lectures will be concentrated mainly on some of the latest experimental contributions, with a view to testing, with high precision, the vacuum polarization effects in muonic atoms predicted by QED.

Although QED in its modern formulation was completed [due to the works of Tomonaga, Schwinger, etc.¹⁾] after the 1950's, some of the ideas introduced had already appeared much earlier: it is interesting to see how some of these new problems were pushed through by the experimental results, even when, owing to the limitations of the available techniques, the measurements sometimes disagreed.

During the period 1932-1938, many spectroscopists²⁾, in various laboratories, noticed that the groups (made up of various lines) H_α , H_β , etc. (D_α , D_β , etc., -- here D stands for deuterium) of the hydrogen were narrower than what would be expected according to the one-particle Dirac theory. The deviations appeared to be very near to the limits of the available techniques, but were consistently present.

[The H_{α} group (H_{β}) is actually composed of all lines corresponding to the transitions from the levels $n=3$ ($n=4$) to the levels with $n=2$ ($n=2$). Therefore, given the one-particle Dirac theory and assuming everything else is known, as for instance the various line intensities, the spectrometer resolution, etc., it was possible to predict the complex shape of the H_{α} (H_{β}) lines].

These measurements, given their important implication, were later repeated, and some contradictory results were obtained, but in 1947 the experimental situation was finally completely clarified with the introduction, by Lamb and Retherford, of a novel technique.

Still, the unexpected results (although often semi-quantitative) of those early experiments (results which today we would qualify as expected), set up a certain amount of speculation in order to try to justify them theoretically, or at least to find out what it was that did not agree with the one-particle Dirac theory of the atom.

Here are some facts worth mentioning, which followed those early spectroscopic observations.

- Bohr and Oppenheimer observed that the levels of the various atoms were calculated without taking into account the interaction between the electromagnetic field (apart from the static potential) and the electron, and that such interaction might have been responsible for the observed differences³⁾. Of course, the trouble was that nobody knew how to calculate the effects of such an interaction.

- In 1933, following a suggestion of M. Born, Kemble and Present⁴⁾ analysed the possibility that the discrepancy might have been due to a finite size of the proton and of the electron. Their conclusion was that the discrepancy was too big to be explained in that way.

- In 1935, Uehling⁵⁾ calculated the correction brought to the Coulomb law by the induced polarization charges due to creation and annihilation of virtual electron-positron pairs within the static electric field of a charge. He found that the Coulomb law was appreciably modified only for distances from charges less than $\lambda_e/2 = 1.9 \times 10^{-11}$ cm. Moreover, he found that this modification was shifting the energy levels by a quantity experimentally unobservable. He also pointed out that in any case the

shift was opposite to the one needed to bring the theoretical predictions into agreement with the experimental results.

- In 1938, Pasternack⁶⁾, analysing the above-mentioned spectroscopic data, came to the following conclusion: to explain the existing discrepancy it was sufficient to hypothesize a shift of the 2S level of about 1000 MHz in the upward direction, i.e. to make the 2S level less bound: no shift for P levels was needed.

- In 1940, Drinkwater et al.⁷⁾, published their results on H_{α} and other lines. The uncorrected experimental results that they found were in agreement, within the experimental errors, with those of Ref. 2; however, they also identified some spurious experimental sources of errors which, according to them, were responsible for the difference between the experimental value and the theoretical expectation (according to the one-particle Dirac theory).

Their results, which cast doubts on the previous published results²⁾, were, as expected, hailed by the theoreticians. At this time there was certainly felt the necessity of including in the calculations of hydrogen atom's levels the effect of the interaction between the electromagnetic field and the electron: unfortunately, all the calculations were giving infinite contributions (and this even for a free electron)*).

- In 1947, after the war, Giulotto again studied the shape of the H_{α} , H_{β} , etc. lines⁸⁾, in part taking into account the findings and criticisms formulated by Drinkwater et al.⁷⁾; he confirmed the existence of the discrepancy in agreement with the authors of Ref. 2.

- In 1947, Lamb and Retherford⁹⁾, taking advantage of the progress obtained during the war in the microwave technique, devised a novel method and measured directly the energy difference $L_1 = 2S_{1/2} - 2P_{1/2}$ and $L_2 = 2P_{3/2} - 2P_{1/2}$. They found the 2S level shifted by 1000 MHz upward, in agreement with Pasternack's conclusion and therefore in disagreement with the one-particle Dirac theory predictions: no shift for P levels was detected.

*) Some feeling for the theoretical situation present during this pre-Lamb period can be grasped from the speech of V. Weisskopf, "My life as a physicist", given in 1971 at Erice, when he spoke about this "Pasternack effect". See, Properties of the fundamental interactions (ed. A. Zichichi) (Editrice Compositori, Bologna, 1973), p. 994.

- Finally, Bethe (1947), introducing for the first time a renormalization procedure in the calculation¹⁰⁾, showed that an upward 2S level shift of about 1000 MHz had to be expected owing to the interaction of the electromagnetic field with the electron.

He obtained this result by defining as observable shift the difference between the shifts calculated for a bound electron and a free electron; all other contributions are according to him already taken into account by taking for the electron mass the experimentally measured value (mass renormalization).

It must be said that Bethe obtained this result in a non-relativistic approximation. An interesting fact is that the observable shift calculated by Bethe turned out to be about proportional to m , where m is the mass of the electron.

- Welton (1948), with an intuitive calculation, has shown that the shift calculated by Bethe can be interpreted as caused by a spread induced in the electron's position by the vacuum fluctuations of the electromagnetic field interacting with the electron¹¹⁾.

- In the following years, Lamb and Retherford¹²⁾, taking full advantage of their novel experimental method, measured the energy level differences L_1 (called the Lamb shift) and L_2 with much greater precision, so that various QED corrections had now to be taken into account to explain the experimental values: it was with this immediate task that QED has been formulated in the early 1950's the way we learn today¹⁾.

- Finally, a very important experimental step was the possibility of the copious production of muons with cyclotrons, and the discovery of X-ray emission observed when negative muons were stopped in various materials¹³⁾. The X-rays originate in the fast de-excitation processes, following the formation of an excited muonic atom which promptly reaches the 1S state.

Since then, coming from the assumption that the muon has no other interactions than electromagnetic and weak ones (an assumption that is well verified by the experimental facts up to now), many different experimental lines involving muons have been used to test various predictions of QED. We recall here some of the most important ones:

i) The study of the hyperfine structure of muonium¹⁴⁾.

- ii) The precise measurement of the $(g-2)_\mu$ of the muon¹⁵⁾; the result of this experiment is one of the most precise tests of QED; also, among all other typical tests, it is the test which involves the highest momentum transfer in the muon-photon interaction.
- iii) The study of the muonic atom energy levels. These measurements are particularly interesting because they can offer a direct test of the electronic vacuum polarization contribution¹⁶⁾ since, for this case, the "Lamb shift" contribution is quite reduced (see next section).

It is clear that in interpreting these types of measurements we can also, when it is possible, remove the assumption that the muon is just a heavy electron and, assuming QED, establish a limit on an eventual new interaction manifested by the muon; for instance, we can give a limit on the strength (or range) of an anomalous muon-hadron interaction (i.e. apart from the electromagnetic and weak ones).

As we already said, these lectures will mainly be devoted to discussing some results obtained in measurements of type (iii) mentioned above.

In studying the muonic energy levels, as in the old spectroscopy, we have two methods:

- 1) Direct measurement of the energy of the X-ray emitted during the transition of the excited muonic atom between the different levels. This method, which was the first applied, is particularly interesting as a test of the electron vacuum polarization when measurements are done in muonic atoms with very high Z (Z being the charge of the nucleus); this is due to the particular resolution properties of the detectors used.
- 2) By using a sufficiently intense tunable electromagnetic radiation, we can induce in a muonic atom (which has first to be prepared in a particular pre-chosen state) a specific transition between two levels; the knowledge of the wavelength at which the transition occurs gives a measurement of the energy difference between the initial and final levels. For technical reasons, this method has so far been applied to the muonic helium ion $(\mu^{-4}\text{He})_{2S}^+$ only.

Of the two methods, I will speak at more length about method (2) since I know more about it.

These lectures contain a second and a third part respectively dedicated to methods (2) and (1), and a fourth part dedicated to the discussions of the results.

In particular, when possible, the two available alternatives mentioned above, will be analysed, i.e. the assumption of a μ -e universality with respect to hadrons and the consequent test of QED, *and vice versa*.

2. VACUUM POLARIZATION EFFECTS IN THE $(\mu^{-4}\text{He})_{2S}^{+}$ IONIC SYSTEM

2.1 Generalities

Soon after that Dirac put forward the first field theory for the electron, it was realized that the vacuum state in the presence of a given "external" electric field would be modified, giving rise to a polarization current (via creation and annihilation of electron pairs); therefore the observable field will be the sum of the original "external" field plus the field created by the polarization charges. For example, taking a point charge (no spin and high mass), the static potential $V(R)$, which is classically described by the Coulomb expression $V_c(R)$, will now be modified by a QED correction.

Let us write it as

$$V(R) = V_c(R) \times [1 + \eta(R)] , \quad (1)$$

R being the distance from the charge and η the polarization charge correction due to the electron field. Actually it should be noted that not only the electron field is present in the vacuum, but all fields associated with possible particles. However, limiting the calculations to distances bigger than or equal to 10^{-13} cm, for as much as we know, the only appreciable contribution to $\eta(R)$ will come from the electron field.

In this case QED gives the following prescription for evaluating the correction:

1) Develop the correction in ascending power of α (fine structure constant):

$$V(R) = V_c(R) \times (1 + \alpha A + \alpha^2 B + \dots) , \quad (2)$$

where to each term of the development there will correspond a definite group of Feynman graphs.

2) With the standard rules of quantum field theory, calculate each term, summing up the contribution of all its graphs. The hope is that each term will come out smaller than the preceding one.

The coefficient A is the one first calculated by Uehling in 1935, and is given by the integral expression [corresponding to graphs (a), Fig. 1]:

$$A = 2/(3\pi) \int_1^{\infty} ds \exp[-2s(r/\lambda)] [1 + 1/(2s^2)] (s^2 - 1)^{1/2} s^{-2} . \quad (3)$$

For the coefficient B we have a similar expression [graph (b), Fig. 1]:

$$B = 2/(3\pi^2) \int_1^{\infty} ds \exp[-2s(r/\lambda)] s^{-1} G(1 - s^{-2}) , \quad (4)$$

where G is a simple but long function calculated first by G. Källén and A. Sabry in 1955, and which can be found in Ref. 17, formula (49):

$$\lambda = \lambda_e = \hbar/m_e c = 3.8 \times 10^{-11} \text{ cm.}$$

Numerical integrations of (3) and (4) give for the correction part $\eta(R)$ (up to α^2) the function of R plotted in Fig. 2¹⁸⁾: we see that $\eta(R)$ is a "short-range" correction with the range

$$r_0 \simeq \lambda_e/2 \quad (5)$$

very near to the Bohr radius of a muonic atom ($Z = 1$) since

$$a_\mu = 2r_0(\alpha f)^{-1} , \quad (6)$$

where f is the ratio of the muon mass to the electron mass. An immediate conclusion is that if we think of a muon bound around such a heavy charged point, its S orbits will be much more affected by the corrective part than the P ones. As an example, in this ideal case considered here the contribution to the 2S-2P energy difference due to the correction considered above will be given by

$$DE_{2S-2P} = \int_0^{\infty} (R_{21}^2 - R_{20}^2) r^2 V_c(r) \times \eta(r) dr , \quad (7)$$

where R_{21} , R_{20} are respectively the radial wave functions of the levels $n = 2$, $\ell = 1$ and $n = 2$, $\ell = 0$ of the muonic atom considered.

The dependence of expression (7) on the mass of the bound particle is much stronger than a linear dependence; therefore it turns out that the Bethe contribution (graph (d), Fig. 1) for the case of the muon is negligible when compared to the contribution of Eq. (7).

In conclusion, a precise measurement of the 2S-2P level energy difference in a muonic atom appears to be an ideal method (at least in principle; in practice we will see what limits it) for checking the QED prediction for the electronic vacuum polarization; in a sense, we can say that this type of measurement is a natural complement of the "Lamb shift" one.

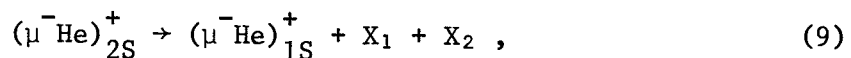
With a view to performing a direct measurement of the 2S-2P energy difference in a muonic atom, in 1970 a group of physicists at the CERN muon channel enquired about the possibility of producing (low-Z) muonic atoms, excited to the 2S level, for a sufficient length of time to be able to perform the necessary measurements on them.

The idea was that once a muonic atom in a 2S level was available in a target for some time, one could try to excite it to the near 2P state, by means of a sufficiently powerful and tunable delayed electromagnetic pulse radiation. The detection of the transition that would eventually occur was thus possible by looking, in coincidence with the radiation pulse, for the typical X-ray emitted due to the very fast decay 2P-1S immediately following the transition (*double resonance method*). The knowledge of the wavelength at which the transition occurred would give a precise indication of the energy difference between the 2S, 2P levels.

A muonic atom in a 2S state (metastable state) is particularly suitable since its spontaneous decay to the lowest 1S level (the 2P one in low-Z muonic atoms is higher than the 2S one) via an electrical dipole transition is forbidden: in general, and always for the case of low-Z muonic atoms, the most probable spontaneous decay (to the lowest level) is via a two-photon emission. The decay rate for such a process $\Lambda_{2\gamma}(Z)$ is given by the expression¹⁹⁾:

$$\Lambda_{2\gamma}(Z) = 10^5 \left(\frac{Z}{2}\right)^6 \text{ sec}^{-1} . \quad (8)$$

For the case in which we are most interested here,



we get a decay rate $\Lambda_{2\gamma}(Z) = 10^5 \text{ sec}^{-1}$: the interesting thing is that $\Lambda_{2\gamma}(Z)$ for low Z is smaller than the free muon decay rate Λ_0 , which is

$$\Lambda_0 = 4.5 \times 10^5 \text{ sec}^{-1} . \quad (10)$$

Using for the first time, at a high-energy accelerator, a high resolution X-ray proportional counter (in the region 1-10 keV) combined with a low-density large target in which negative muons could be stopped at a relatively high rate, a CERN-Pisa Collaboration studied both the prompt and the delayed X-ray emission following the stopping of muons in hydrogen and helium^{19,20}.

From this experimental study it was possible to prove directly¹⁹⁾ the formation of the 2S metastable system $(\mu^{-4}\text{He})_{2S}^{+}$. By observing the X-rays coming from the rare decay^{7,19)} it was found that 4% of the negative muons stopped in pure helium gas at a few atm were indeed reaching the metastable level 2S. In a subsequent measurement^{21,22)} the total disappearance rate λ of the $(\mu^{-4}\text{He})_{2S}^{+}$ system was measured for the case in which muons were stopped in helium gas at pressures ranging from 10 to 50 atm; it was found that once formed, the 2S system would live for about 1.6 μsec . Table 1 gives the total disappearance rate as well as the different partial disappearance rates as function of the pressure of the target within which the $(\mu^{-4}\text{He})_{2S}^{+}$ system is formed.

We can see that, probably after 50 atm (300 K), de-excitation of the 2S state to the 1S via Stark and Auger processes becomes appreciable.

The problem of finding experimentally the disappearance rate of the metastable neutral muonic atom $(\mu^{-}\text{P})_{2S}$ formed by stopping muons in hydrogen (which should initially be formed in about 8% of the cases) has not yet been solved.

There is one important remark to be made; from the experimental results of Table 1, we deduce that the metastable muonic system $(\mu^{-4}\text{He})_{2S}^{+}$ remains for most of its existence as an ion. In fact we can now easily understand it, since a transfer of an electron from a helium atom, during a collision, to the ionic $(\mu^{-}\text{He})^{+}$ system cannot occur because it is energetically impossible. This fact is a rather crucial one, because when the 2S metastable ion $(\mu^{-4}\text{He})_{2S}^{+}$ catches an electron it will, in a few nano-seconds, make the jump from 2S to 1S, ejecting the electron (Auger effect); this suggests that the helium target has to be clear of other gases.

As a consequence of these findings, in 1972 a CERN-Pisa-Bologna-Saclay Collaboration decided to try to perform the double resonance experiment,

outlined above, in order to measure the energy difference between the 2S-2P levels. For technical reasons it was decided to start by searching for the $2S_{1/2}-2P_{3/2}$ line.

Figure 3 shows the diagram of the first lower levels of the $(\mu^{-4}\text{He})^+$ system. In the following we will define $S_1 = 2S_{1/2} - 2P_{1/2}$ and $S_2 = 2S_{1/2} - 2P_{3/2}$.

Table 2 gives the theoretical predictions for S_1 and S_2 ²³⁾ according to the latest analysis of Rinker ²⁴⁾. From this table we see that

- i) a non-negligible contribution to S_1 and S_2 is given by the effect of the helium nucleus size; in fact the error on the prediction is essentially due to the uncertainty in the helium (r.m.s.) charge radius ²⁵⁾;
- ii) as expected, the electronic vacuum polarization contribution is the dominant term and the Lamb-shift one is quite small. The contribution to the electronic vacuum polarization shift coming from the α^2 term [see formula (2)] is about 2.8 times the calculated uncertainty on S_1 and S_2 . The muon vacuum polarization is negligible.

The natural widths Γ of the S_1 and S_2 lines are determined by the lifetime of the 2P level T: since $T = 5 \times 10^{-13}$ sec, we get

$$\Gamma = 8 \text{ \AA} . \quad (11)$$

Looking at Table 2 we see that the electromagnetic radiation necessary to induce a 2S-2P transition in a $(\mu^{-4}\text{He})^+_{2S}$ system is in the near-infrared region: this fact is very important since there exists a type of laser (the dye laser) which can yield infrared-light short pulses, within the region 6000-10000 Å, which are quite energetic (a fraction of a joule) and which can be made tunable. According to the method used and the wavelength interval needed, a specific dye must be chosen with the relative solvent.

A first set-up to perform ²⁶⁾ the measurement of S_2 , employing a specially developed, powerful, tunable dye laser was constructed and brought into operation in 1972; in 1973 was obtained the first evidence that a 2S-2P transition could be induced via laser excitation ²⁷⁾. In 1975, after the CERN Synchro-cyclotron was modified, the measurements were repeated with improved apparatus, and it is the performance and the results of this last experiment which I am going to briefly describe.

2.2 The experiment^{26,28)}

The measurement was performed stopping negative muons from the CERN Synchro-cyclotron in a target filled with ${}^4\text{He}$ at 40 atm ($T = 293$ K). As we said, about 4% of the muons actually stopped in gas form the metastable $(\mu^{-4}\text{He})_{2S}^+$ system (lifetime ~ 1.6 μsec). A short time (~ 0.5 μsec) after the stop, an energetic pulse of laser light was sent into the target to excite the $2S_{1/2} \rightarrow 2P_{3/2}$ transition. The laser was tuned across the resonance line, and the eventual transition identified by detecting with NaI crystals, in coincidence with the laser pulse, the 8.2 keV X-ray emitted in the fast $2P_{3/2} \rightarrow 1S_{1/2}$ decay.

The schematic arrangement of the apparatus is shown in Fig. 4: a telescope of plastic scintillation counters defines the incoming muon beam, which is slowed down by suitable CH_2 moderators. The last telescope counter is a thin plastic scintillator mounted inside the target vessel. Eight NaI(Tl) counters (A_1, \dots, A_8) were used to anticoincide the muon beam and to detect the 8.2 keV muonic X-rays. In order to avoid spurious signals from the laser light, the A_i counters' photomultipliers were coupled to the light-guides through Corning CS 4.97 blue filters (attenuation factor $> 4 \times 10^4$ for the laser light to be used).

A useful cylindrical stopping region V (14 cm long and 4 cm in diameter) was defined inside the target itself (see Fig. 1) by a 12 μm thick Al foil, internally gold-coated (400 \AA), in order to ensure maximum reflectivity for the laser light.

The light entered the target vessel through an antireflecting window W: 6 mm diameter holes were provided in the Al foil and in the anticoincidence counter 5 closing the region V. To ensure the entering of the light in the region V, an internally gold-coated thin metal conic tube C drove the laser light through the holes.

The light source was a dye laser pumped by a Q-switched ruby laser: in the following brief description of the laser system is given.

The ruby laser is composed of a head containing the ruby rod ($\frac{5}{8}$ inch diameter and 6 inches long) and the helical flash, plus, in line with the optical axis, a Q-switch; the cavity is defined by two reflecting mirrors, the exit one having a transmission coefficient of 30%.

The Q-switch, which is composed of a Pockel cell plus a polarizer, is usually in an open condition (the ruby rod cannot lase); by using a proper fast electrical pulse, it can be put into a closed condition, after which in a few tens of nanoseconds the ruby will lase.

The dye used in the present apparatus is polymethine dye (called HITC) from which infrared radiation covering the 8040-8180 Å wavelength range can be obtained with high efficiency by pumping with a Q-switched ruby laser. The HITC is dissolved in dimethylsulfoxide (DMSO), since such a solvent increases the lasing efficiency of polymethine dyes.

The liquid solution of HITC dye in DMSO has a molar concentration of about 5×10^{-5} , and a total volume of 130 cm³, including a small reservoir to allow for cooling and circulation of the liquid. The solution is contained in an 11 mm optical path cell, having two quartz windows 10 mm thick and 5.08 cm in diameter; these windows are provided with broad-band antireflecting coating.

A centrifugal pump keeps the solution in continuous circulation within the cell.

The dye laser cavity (see Fig. 4) is made of a diffraction grating (DG) and a dielectric mirror (M) with 30% reflectivity in the useful wavelength range; the dye cell is placed between them. The mirror and the grating are spaced 80 cm apart.

Proper orientation of the grating makes the first-order diffraction of the chosen wavelength λ to come back upon itself along the axis of the optical cavity.

In this way the wavelength of the output radiation from the dye laser was tuned to a particular value λ contained in the region 8040-8180 Å (for the case of HITC); λ is then varied by rotating the grating (DG).

Remote-controlled tuning was provided, the diffracting grating (DG) being driven by a stepping motor (SM) (see Fig. 4). Each motor step corresponded to a 2.2 Å change of the laser wavelength. The motor was linked to a HP 2100 computer via a CAMAC interface. The calibration of the stepping motor was performed using a digitized spectrometer (2 Å steps), the scale of which was fixed using as a reference the two lines of an Ar lamp, $\lambda_1 = 8115.3 \text{ Å}$ and $\lambda_2 = 8103.7 \text{ Å}$. The stability of the spectrometer was found to be better than 1 Å over the data-taking period.

The repetition rate of the laser system was 0.25 Hz.

It should be noted that the time necessary to pump the ruby rod above the critical inversion is about 2 msec, which is much too long when compared to τ_{2S} . For this reason it is impossible to trigger the pumping flash lamp directly with a signal given by the incoming muon.

On the other hand, for the ruby laser, it was verified that the critical inversion (lasing conditions) lasted for a time interval of 1 msec; therefore a fairly long time interval was available, within which, by closing the Q-switch by means of a trigger signal, the ruby laser system would be able to lase.

For these reasons a technique which synchronized the trigger of the flash lamp with the muons entering the target (which for this experiment were bunched in bunches of a few milliseconds) was developed. The sequence of the different steps is given below:

- i) The synco-cyclotron accumulates about 20 bunches of protons (each 0.2 msec wide) at a definite radius. During this storage time, the internal target is set at a few centimetres below the median beam plane, in such a way that it does not interact appreciably with the accumulating beam.
- ii) The internal target then flips across the region of the stored beam at a time τ_T (maximum target speed: 1 cm/msec). This gives rise to a muon bunch which is observed by the present apparatus to be about 3-5 msec with no significant microstructure. The electronic trigger system is arranged so that muons are accepted only in a time interval (Δt) of 1 msec centred in the 3-5 msec bunch.
- iii) At a time τ_F , 2 msec before the interval Δt , the flash lamp of the ruby is discharged, thus energizing the ruby rod: during this operation the Q-switch is kept open. The time τ_F is so chosen that at the beginning of the time interval Δt (when the stopping muons are accepted by the trigger electronics) the ruby rod is ready to lase.
- iv) The first MUSTOP signal, registered by the electronics within the 1 msec interval Δt , closes the Q-switch (time τ_P) starting the lasing action. The general characteristics of the dye laser are given in Table 3.

A MUSTOP signal = $\overline{12345} \overline{\Sigma A_i}$ (see Fig. 4) identified the stopping muon; this signal generated

- i) a prompt 2 μ sec wide gate signal G; during this gate time the first pulse P_i given by each of the eight A_i counters was signalled (if present);
- ii) a 0.5 μ sec delayed trigger pulse to the ruby laser Q-switch;
- iii) a properly delayed signal which, at the end of the event, triggered the data acquisition process.

Among others the following relevant data were recorded, for each event, on magnetic tape via the HP 2100 computer:

- i) the integrated amplitudes and the times of all signalled pulses P_i ;
- ii) the stepping motor position (SMP), the reading of the spectrometer, and the energy E and time t_1 of the laser pulse.

All times were measured with respect to the MUSTOP signal.

After completion of the data acquisition period, the dye laser wavelength was changed by 2.2 \AA via the SM.

An interval of about 38 \AA , centred at about 8117 \AA , was continuously spanned backwards and forwards, the entire range being swept in about three minutes. It should be remembered that in the first measurement of the $S_2 = 2S_{1/2} - 2P_{3/2}$ splitting, the value²⁷⁾ 1527.4 ± 0.9 meV was obtained, which in wavelength reads $\lambda'_0 = 8117 \pm 5$ \AA .

The main result is presented in Fig. 5. On the ordinate is given the number of events detected, in a time interval of 250 nsec from the laser time t_1 , by the eight A_i counters as a function of the SMP spanned during the experiment. The wavelength scale shown on the abscissa is obtained from the calibration.

The full-line curve drawn through the data points represents the best fit ($\chi^2 = 11$) with a Lorentzian line plus a constant background contribution; in the fit, the width Γ (FWHM) of the Lorentzian curve was fixed at the value $\Gamma = 8$ \AA , which represents the theoretical width for S_2 . The wavelength value λ_0 of the centre of the Lorentzian line, according to the best fit, is

$$\lambda_0 = 8116.8 \pm 1.5 \text{ \AA} \quad (12)$$

which, expressed in meV, is

$$S_2^{\text{exp}} = 1527.5 \pm 0.3 \text{ meV} . \quad (13)$$

The error quoted includes the statistical error as well as the uncertainty in the spectrometer calibration. The number of events in the peak given by the best fit is 233 ± 45 , and the signal-to-background ratio at the peak is 1.04. A fit with only a straight line (no effect) gives $\chi^2 = 38$. The number of events found is in agreement with the expected one.

3. ON X-RAYS EMITTED FROM HEAVY MUONIC ATOMS

I will not talk at length about this topic; I wish only to recall some of the results in this field in order to complete the discussion on those subjects which will be raised when discussing the results obtained for the $(\mu^{-4}\text{He})^+$ system previously presented.

As already pointed out, in this case the X-ray energies are directly measured: this is done by means of a solid-state detector [Ge(Li)]. The resolution that can be obtained is, for the X-rays energies around 450 keV, about (HWMH) 1.5 keV: the results indicate that in these conditions it is possible to locate the peak position to about 1% (or better) of the width. It is clear that an important part of the measurements is the absolute calibration. In Fig. 6 a typical set-up is shown [taken from the forthcoming publication by Tauscher et al.²⁹⁾].

Many types of interesting information can be obtained from precise measurements of these X-ray energies; those most relevant to our purpose are described in the two following sections.

3.1 Electronic vacuum polarization effects

There are at least the following reasons why this method is, in this case, interesting:

- a) The momentum transfer involved in the muon-nucleus electromagnetic interaction is $Z\alpha m_{\mu} c$: therefore this is quite high.
- b) With this method the check of the vacuum polarization effects is virtually independent of the exact knowledge of the nucleus form factor

(although there are other limitations); thus one type of systematic error present in the previous experiment (Section 2) is absent here. (In particular, a short-range muon-hadron anomalous interaction does not contribute to the shift.)

- c) The electronic vacuum polarization effects that can be detected here are those given by graphs (a), (b) and (c) of Fig. 1; it has to be noticed that information on the last graph cannot be obtained from measurements on light muonic atoms, where its contribution is negligible. Let me point out that the process characterized by graph (c), Fig. 1 represents a non-linear behaviour of the electromagnetic field: this is another characteristic consequence of QED which was not envisaged by the Maxwell-Lorentz electrodynamics (photon-photon interaction).

The first precise experimental study of this type was done by Backenstoss et al. at the CERN muon channel in 1969. Up to 1974 the situation was a little confused owing to the uncertainties in the theoretical predictions and to the fact that some published data did not agree. Now there seems to be agreement everywhere. Some of the main results are presented in Fig. 7 (this figure has kindly been given to me by Professor L. Schellenberg). In this figure the data of Tauscher et al. are not the final ones; the final results will be presented in Ref. 29, but they do not change appreciably. From Ref. 29 I have taken their theoretical estimates of the lines observed by them, and have put them on Fig. 7.

In order to see how the different errors are estimated, I have also copied from Ref. 29 the list of the different contributions to the shifts and the theoretical errors as estimated by them (see Table 4).

3.2 Precise determination of the r.m.s. charge radius $\langle r^2 \rangle_{\mu}^{\frac{1}{2}}$ of the nucleus involved

This is an interesting field by itself, but we mention it here with a view to comparing it with the corresponding r.m.s. charge radius $\langle r^2 \rangle_e^{\frac{1}{2}}$, as obtained in electron-nucleus scattering experiments. This comparison is interesting because the difference E,

$$E = \langle r^2 \rangle_{\mu}^{\frac{1}{2}} - \langle r^2 \rangle_e^{\frac{1}{2}}, \quad (14)$$

can set a direct constraint to the presence of an anomalous muon-hadron interaction (μ -e universality); there are many heavy nuclei for which E

is known with a precision comparable to the one with which E is deduced from high-energy muon-proton scattering.

The new and interesting fact with heavy nuclei is that here, to such an anomalous muon-hadron interaction, there contribute (enhancing it) many nucleons, and moreover a different mixture of protons and neutrons is in principle available (this is important in case the anomalous muon-hadron interaction would have an isospin dependence). This comparison has been done by Rinker and Wilets³⁰⁾, and their results are presented in Table 5 together with other similar observations. Let me add that in order to make such a comparison, a correction due to the nuclear polarizability³⁰⁾, for the case of the r.m.s. deduced from muonic X-ray data, has to be applied. Moreover, the different values of $\langle r \rangle_e^{\frac{1}{2}}$ are deduced after normalizing all scattering electron-nucleus cross-sections used (for the case shown in Table 5) to the ^{12}C electron scattering cross-section, which is used as the "standard" one: unfortunately there exist two measurements of this "standard" cross-section and they are not in a good agreement with one another. For the results presented in Table 5 the latest measurements of the electron- ^{12}C nucleus scattering cross-section have been used (see the discussion in Ref. 30).

4. DISCUSSION OF THE RESULTS

4.1 QED tests

From the work of Sick et al.²⁵⁾, for the helium r.m.s. charge radius we get the value

$$\langle r \rangle_e^{\frac{1}{2}} = 1.674 \pm 0.012 \text{ fm} . \quad (15)$$

The error given in Eq. (15) has been deduced from a maximum dispersion obtained in the analysis procedure; the statistical errors are negligible.

Using the calculation results of Rinker²⁴⁾ (see Table 2) together with the value (15) and the experimental value (13), we obtain for the difference D ,

$$D = S_2^{\text{exp}} - S_2^{\text{theor}} = 0.2 \pm 4.2 \text{ meV} . \quad (16)$$

The errors due to the experimental measurements (0.3 meV) and the errors due to the uncertainty in the calculations (1.12 meV) are much smaller than the error introduced by the uncertainty in the value (15) for $\langle r \rangle_e^{\frac{1}{2}}$.

Referring to the QED prediction, we see that (with a 95% confidence level) this is verified to 0.25%; moreover, we can say that the vacuum polarization shift due to the term in α^2 [see formula (2) and graphs (b) and (c) of Fig. 1] is verified to about 35%.

Concluding, the results of Eq. (16) make us believe that the Coulomb static potential around a charge ($Z = 1$) is modified by the vacuum polarization as QED demands; as an exercise let us assume that QED is formally valid (with the vacuum polarization contribution given mainly by a Dirac charged particle of mass m), and try with the results of (16) to deduce the mass (and therefore the range $r_0 = \pi/2mc$) which enters in the corrective term $\eta(R)$ of formula (1). We get [see formula (3)]

$$m = 0.5110 \pm 0.0020 \text{ MeV} , \quad (17)$$

i.e. we find that these *virtual particles* appear with a mass equal to the (renormalized) mass of the electrons.

Conversely, fixing the range r_0 (or the mass of the virtual pair) we can deduce the value of the coupling α_V with which this pair couple with the photon. For instance [considering only the first term in formula (2)], we find for α_V , which multiplies the coefficient A, that it is equal to α (of the Rosenfeld table) within a few per thousand. To put these results in another direct way, we can say, from this direct test of QED (see beginning of Section 2.2.1), that another non-"strongly interacting" charged particle with a mass smaller than (or around) the electron mass *cannot* exist; vice versa, a non-strongly interacting particle with mass equal to that of the electron has to have a coupling α (that is, charge e) or a much smaller one.

Let us now look at the results of the high-Z muonic atoms. From Fig. 7 we see that indeed the dispersion of the various experimental results is in good agreement with the experimental errors ascribed to them. Considering the spread of the different experimental data and of the theoretical predictions, it seems fair to accept the opinion of the experts, that there is agreement between theory and experiment at the level of 0.4%. It is an important step that an agreement at this level is obtained also at rather high momentum transfer.

The photon-photon interaction [graph (c), Fig. 1] contribution is checked to about 20% *).

The results given above have already been anticipated in part by the results of the "Lamb shift" in normal hydrogen: it should, however, be remembered that in that experiment the momentum transfer is αm_e and therefore quite small (see Table 6). We feel that now *direct* tests have been done *within* the correction range r_0 , the agreement to a few per thousand (at least) can safely be accepted (see Fig. 1).

Concluding this topic we present Table 6, where the results of the most precise vacuum polarization experiments are given, and from which we can see that, for the electronic vacuum polarization test, the measurement of the $2S_{1/2} - 2P_{3/2}$ difference in the $(\mu^{-4}\text{He})^+$ system gives the most precise test so far available.

4.2 Muon-hadron anomalous interaction

There are many experimental tests on μ -e universality³¹⁾, some of which are rather precise. However, for reasons of homogeneity in the data, here we will consider only those tests extracted from nucleon-lepton elastic interactions. As already pointed out, QED is here assumed to be valid.

Using the prediction of Rinker (see Table 2), from the results (13) we get for the r.m.s. of the helium charge radius, as seen by the muon, the value

$$\langle r^2 \rangle_{\mu}^{\frac{1}{2}} = 1.6733 \pm 0.0030 \text{ fm} . \quad (18)$$

The error given is determined by the experimental error and by the calculation error.

Taking the value given by Sick et al.²⁵⁾ [see equality (15)], we obtain

$$E = \langle r \rangle_{\mu}^{\frac{1}{2}} - \langle r \rangle_e^{\frac{1}{2}} = 0.0007 \pm 0.012 \text{ fm} . \quad (19)$$

These results were determined with an uncertainty similar to the one with which the equivalent \bar{E} (averaged over different nuclei) has been determined by Rinker and Wilets³⁰⁾ (see Table 5). For comparison we have also put in Table 5 the results deduced from high-energy μ -p elastic scattering (which have been done for a range of momentum transfer up to $5.5 \text{ GeV}/c$)³²⁾.

*) If one assumes everything else known the latest experimental result of the $(g-2)_{\mu}$ experiment checks the theoretical photon-photon contribution to about $\pm 5\%$.

It is clear that the limits found for the different E's of Table 5 are very similar; however, we should remember that for the case of the nuclei (where A is rather big), at least for certain hypothetical cases, the level of sensitivity for detecting a muon-hadron anomalous interaction should be enhanced.

In order to understand the meaning of a limitation of the type (19), let us discuss this case ($Z = 2$, $A = 4$) as an exercise. It is possible to show that in this case, if there is a vector particle of mass M mediating an anomalous interaction between the hadrons and the muon with couplings f_1 and f_2 respectively with the muon and the hadron, we can write

$$E = \frac{f_1 f_2}{M^2} \times \frac{6}{\alpha \langle r \rangle_e^2} \quad (20)$$

which, inserting the various values, gives (M in MeV)

$$\frac{f_1 f_2}{M^2} < 6.1 \times 10^{-10}. \quad (21)$$

So if $f_1^2 = f_2^2 = \alpha$, we get $M \gtrsim 3.3$ GeV: on the other hand, putting $f_1^2 = f_2^2 = f^2$ and $M = m_\pi$ we get $f^2 < 1.6 \times 10^{-3} \alpha$.

Moreover, taking the latest results obtained in the $(g-2)_\mu$ experiment, we can give the limit³³⁾

$$\left(\frac{f_1}{M} \right)^2 < 3 \times 10^{-11}. \quad (22)$$

It may be interesting at this point to see the case in which we assign to f_2^2 the same value of the ρ -nucleon coupling constant (~ 2); from formulae (21) and (22) we have

$$f_1^2 < 3 \times 10^{-11} M^2; \quad f_1^2 < 1.9 \times 10^{-19} M^4. \quad (23)$$

At the value of $M \approx 12$ GeV, the two limits coincide, fixing for f_1^2 the value $\sim \alpha/2$. One conclusion from (23) is that the existence of a vector particle with mass ~ 4 GeV strongly coupled with hadrons and coupled with muons with a coupling constant about $10^{-2} \alpha$, cannot be ruled out by the experimental data presented here (a somewhat better limit can be obtained from the deep inelastic μ -p scattering results of Ref. 32). For other detailed discussions on this subject see the analysis of Barshay³⁴⁾ and Barbieri³⁵⁾.

5. CONCLUSIONS

We have seen that for checking the QED vacuum polarization effects, the "laser spectroscopy" applied to the muonic system gives at present the most precise test; moreover, it remains quite promising for the future. It is not limited by the experimental techniques nor by the theoretical estimate, but at present by the knowledge of the nucleus form factor; how to avoid this "accident" is the next task of this new branch of investigation.

Regarding the search for an anomalous muon-hadron interaction using results from muonic atoms, we can say that at present we are much more limited by the inaccuracy of the present electron-nuclei scattering experiments.

Acknowledgements

I would like to thank Prof. J. Bell for advice and criticism given not only while reading this lecture but also during all the experimental activities since the beginning of this experimental line.

REFERENCES

- 1) See, for instance, J. Schwinger, Quantum Electrodynamics (Dover Publ. Inc., New York, NY, 1958).
- 2) W.V. Houston, *Astrophys. J.* 64, 81 (1926).
Kent-Taylor and Pearson, *Phys. Rev.* 30, 266 (1930).
W.V. Houston and Y.M. Hsieh, *Phys. Rev.* 45, 263 (1934).
R.C. Williams and R.C. Gibbs, *Phys. Rev.* 45, 475 (1934).
Kopfermann, *Naturwissenschaften* 22, 218 (1934).
F.H. Spedding, C.D. Shane and N.S. Grace, *Phys. Rev.* 47, 38 (1935).
R.C. Williams, *Phys. Rev.* 54, 558 (1938).
W.V. Houston, *Phys. Rev.* 51, 446 (1937).
- 3) See, W.V. Houston and Y.M. Hsieh of Ref. 1.
- 4) E.C. Kemble and R.D. Present, *Phys. Rev.* 44, 1031 (1933).
- 5) E.A. Uehling, *Phys. Rev.* 48, 55 (1935).
- 6) S. Pasternack, *Phys. Rev.* 54, 1113 (1938).
- 7) J.W. Drinkwater, O. Richardson and W.E. Williams, *Proc. Roy. Soc.* 174, 164 (1940).
- 8) L. Giulotto, *Phys. Rev.* 71, 562 (1947); *Ricerca Scient.* 17, 209 (1947).
- 9) W.E. Lamb and R.C. Retherford, *Phys. Rev.* 72, 241 (1947).
- 10) H. Bethe, *Phys. Rev.* 72, 339 (1947).
- 11) T.A. Welton, *Phys. Rev.* 74, 1157 (1948).
- 12) See review of W.E. Lamb, *Rep. Progr. Phys.* 14, 19 (1951).
- 13) V.L. Fitch and J. Rainwater, *Phys. Rev.* 92, 789 (1953).
- 14) V.W. Hughes et al., *Phys. Rev. Letters* 5, 63 (1960).
- 15) J. Bailey et al., *Phys. Letters* 55B, 420 (1975).
- 16) This was first realized by S. Koslov, V.L. Fitch and J. Rainwater, *Phys. Rev.* 95, 291 (1954).
- 17) G. Källén and A. Sabry, *K. Danske Vidensk. Selsk. Mat.-Fys. Medd.* 29, 17 (1955).
- 18) E. Zavattini, On the 2S-2P energy difference in very light muonic systems, *Lecture Notes in Physics (Laser spectroscopy)* (Springer-Verlag, Berlin, 1975), Vol. 43, p. 370.
- 19) A. Placci et al., *Nuovo Cimento* 1A, 445 (1971).
- 20) A. Placci et al., *Nuclear Instrum. Methods* 91, 417 (1971).

- 21) A. Bertin et al., Nuovo Cimento 26B, 433 (1975).
- 22) A (rare) second-order e.m. process like (9) but for normal helium has been observed in 1965 by M. Lipeless et al., Phys. Rev. Letters 15, 690 (1965).
- 23) For the equivalent figure for $(\mu^{-3}\text{He})^+$, $(\mu^{-}\text{P})$, and $(\mu^{-}\text{D})$ systems, see Ref. 18 and references therein.
- 24) G. Rinker, Phys. Rev. 14A, 18 (1976).
- 25) I. Sick, J.S. McCarthy and R.R. Whitney, Phys. Letters 64B, 33 (1976).
- 26) A. Bertin et al., Nuovo Cimento 23B, 489 (1974).
- 27) A. Bertin et al., Phys. Letters 55B, 411 (1975).
- 28) G. Carboni et al., Precise measurement of the $2S_{1/2}-2P_{3/2}$ splitting in the $(\mu^{-4}\text{He})^+$ muonic atom, Nuclear Phys. A278, 381 (1977).
- 29) L. Tauscher et al., Precision measurements of the muonic 5-4 transitions in Pb and 4-3 transitions in Ba as test of the validity of QED, to be published. (I thank Dr. L. Tauscher for giving me a copy of this forthcoming publication.)
- 30) G.A. Rinker, Jr. and L. Willets, Phys. Rev. D 7, 2629 (1973).
- 31) A. Eutenberg et al., Phys. Rev. Letters 32, 486 (1974).
- 32) I. Koustalos et al., Phys. Rev. Letters 32, 489 (1973): in particular, see discussion by these authors.
- 33) F. Combley and E. Picasso, Some topics in QED Lectures given at the Internat. School of Physics "E. Fermi" on Metrology and Fundamental Constants; Varenna, July 1976.
- 34) S. Barshay, Phys. Rev. D 7, 2635 (1973).
- 35) R. Barbieri, CERN-TH 1963 (1975).

Table 1

Disappearance channels for the $(\mu\text{He})_{2S}^+$ system and corresponding rates^{a)}

Process	Symbol	Rate (sec^{-1})
Muon decay	λ_0	4.54×10^5
Muon capture	λ_c	45 ± 5
Two-quantum decay	λ_{2X} ^{b)}	1.06×10^5
Spontaneous M1 transition ^{c)}	λ_{M1}	0.53
Total disappearance rate at zero density	$\lambda_{2S,tot}(0 \text{ atm}) =$ $= \lambda_0 + \lambda_c + \lambda_{2X} + \lambda_{M1}$	5.6×10^5
External Auger effect	$\lambda_A(P)$	$(2.4 \pm 1.4) \times 10^3 \times P$ ^{d)}
Stark-mixing collisions	$\lambda_{St}(P)$	$\leq 300 \times P$
Total disappearance rate at pressure P	$\lambda_{2S,tot}(P) =$ $= \lambda_{2S,tot}(0 \text{ atm}) + \lambda_A(P) + \lambda_{St}(P)$	

a) Taken from Ref. 21.

b) This process occurs via the emission of two X-rays; the sum of their energies is 8.2 keV.

c) This process yields the emission of an 8.2 keV X-ray.

d) P is the helium pressure in atmospheres.

Table 2

Contribution^{a)} to the energy difference between the 2S and 2P levels in the $(\mu^{-4}\text{He})^{+}$ system ($Z = 2$). Taken from Ref. 24. Energies in meV; $\langle r^2 \rangle$ charge r.m.s. radius of helium in fm^2 .

Contributions		$S_1 = 2P_{1/2} - 2S_{1/2}$	$S_2 = 2P_{3/2} - 2S_{1/2}$
Electronic vacuum polarization	Uehling terms $\propto (\alpha Z)$	1599.8	1666.1
	Källén-Sabry terms $\propto \alpha^2 (\alpha Z)$	11.6	11.6
Muon vacuum polarization	$\alpha(\alpha Z)$	-	0.3
Recoil		0.3	0.3
Nuclear polarizability		3.1	3.1
Fine structure		-	145.6
Finite size corrections		$-3.1-102.0 \langle r^2 \rangle$	$-3.1-102.0 \langle r^2 \rangle$
Vertex correction	$\alpha(\alpha Z)$	-10.9	-10.6
	$\alpha(\alpha Z)^2$	-0.2	-0.2
Total in meV ^{b)}		$1666.9-102.0 \langle r^2 \rangle$	$1813.1-102.0 \langle r^2 \rangle$
Total in meV ^{c)}		1381.7 ± 4.2	1527.3 ± 4.2
Total in angstrom ^{d)} (Å)		8973.5 ± 21.8	8118 ± 21.8

a) The contribution due to weak interaction is $\approx 2 \times 10^{-5}$ meV; J. Bernabeu et al., CERN TH-1853 (1974).

b) The theoretical uncertainty is ± 1.1 meV and comes mostly from the uncertainty of the nuclear polarization contribution.

c) $\langle r^2 \rangle$ taken from Ref. 25; the error given here also takes into account the uncertainty with which $\langle r^2 \rangle$ is given.

d) The natural width of S_1 and S_2 is $\Gamma \approx 8 \text{ Å}$.

Table 3

Characteristics of the dye laser used in the present apparatus

Dye	HITC ^{a)}
Solvent	DMSO ^{b)}
Molar concentration (moles/litre)	$\sim 5 \times 10^{-5}$
Average ruby pumping energy (J)	1.2
Average pulsed infrared output energy (mJ)	270
Radiation pulse duration (nsec)	~ 20

a) 1,3,3,1',3'-Hexamethyl-2,2'-indotricarbocyanine iodide:
purchased from K & K Labs., Plainview, NY, USA.

b) Dimethylsulfoxide: purchased from Carl Bittman A.G.,
Basel, Switzerland.

Table 4

Calculations and comparison with experimental values in eV

	Pb		Ba	
	$5g_{9/2} \rightarrow 4f_{7/2}$	$5g_{7/2} \rightarrow 4f_{5/2}$	$4f_{7/2} \rightarrow 3d_{5/2}$	$4f_{5/2} \rightarrow 3d_{3/2}$
E_0 a,b)	429'334.1	435'663.7	431'590.2 (1.0)	438'933.9 (3.0)
Recoil	2.2	2.2	3.6	3.7
Nuclear polarization	4.5 (0.5)	5.0 (0.5)	7.9 (0.8)	9.5 (1.0)
Electron screening	-75.7 (7.0) c)	-75.7 (7.0) c)	-12.9 (2.5) d)	-12.9 (2.5) d)
$\alpha(\alpha Z)$ b,e)	2105.0 (1.0)	2188.8 (1.0)	2327.5 (1.0)	2434.5 (1.0)
$\alpha^2(\alpha Z)$ b)	14.5	15.1	16.2	17.0
$\alpha(\alpha Z)^{n \geq 3}$ b)	-42.0 (2.0)	-42.0 (2.0)	-19.0 (1.0)	-19.0 (1.0)
$\alpha^2(\alpha Z)^2$	1.2	1.2	1.0	1.0
Self energy	-0.9	-0.9	-1.5	-1.5
E^{th}	$431'343 \pm 7$	$437'757 \pm 7$	$433'913 \pm 3$	$441'366 \pm 4$
E^{exp}	$431'359 \pm 11$	$437'747 \pm 12$	$433'925 \pm 8$	$441'373 \pm 9$
$E^{\text{th}} - E^{\text{exp}}$	-16 ± 13	10 ± 14	-12 ± 9	-7 ± 10
$\langle E^{\text{th}} - E^{\text{exp}} \rangle$	-8 ± 6			

a) Contains anomalous magnetic moment.

b) Contains finite size contribution.

c) 1.8 ± 0.2 K-electrons, 6 L-electrons.

d) 1.4 ± 0.3 K-electrons, 6 L-electrons.

e) Contains ladder graphs.

All calculations are done for extended nuclear charge.

Table 5

Comparison of the nuclear charge radius (for some nuclei) obtained by muonic atomic studies ($\langle r \rangle_{\mu}^{1/2}$) and by electron scattering results ($\langle r \rangle_e^{1/2}$);
 $E_i = \langle r \rangle_{\mu}^{1/2} - \langle r \rangle_e^{1/2}$

Z	A	E_i in fm
1	1	≤ 0.013 a)
2	4	$+0.0007 \pm 0.012$ b)
13	27	} weighted average -0.002 ± 0.014 c)
14	28.086	
20	40	
22	47.90	
28	58.71	
29	63.456	

a) Taken from Ref. 30.

b) Formula (19), this lecture.

c) Taken from Ref. 29 (using the data of the Amsterdam group on ^{12}C -electron elastic scattering data).

Table 6

Comparison between theory and experiment on vacuum polarization

Experiment	Total effect (theory)	Vacuum pol. (theory)	Exp. value	Accuracy of vac. pol. test (\pm) ϵ	Momentum transfer ^{a)}
g-2/electron ^{b)}	115965.25×10^{-8}	9.4×10^{-8}	$(115965.67 \pm 0.35) \times 10^{-8}$	3.7%	cm_e^c
g-2/muon ^{b)}	1165921×10^{-8}	585.6×10^{-8}	$(1165922 \pm 0.9) \times 10^{-8}$	0.17% ^{b)}	m_μ^c
Lamb shift (H) ^{c)}	1057.916 MHz	27.323 MHz	1057.893 ± 0.020 MHz	0.07% ^{c)} (0.3%)	cm_e^c
$2P_{3/2} - 2S_{1/2}$ in (μHe) ^{d)}	1.5274 eV	1.6774 eV	1.5275 ± 0.0003 eV	0.25% ^{e)}	cm_μ^c
High-Z muonic atoms ^{f)}	~ 430000 eV	~ 2100 eV	see Fig. 7	0.4%	$\alpha Z m_\mu^c$

a) m_e and m_μ are the electron and muon masses, respectively; α is the fine structure constant.

b) Here we have taken the combined results on μ^+ and μ^- ; see J. Bailey et al., The anomalous magnetic moment of positive and negative muons, CERN preprint (to be published in Phys. Letters B), 8 February 1977. We have considered here only the experimental error: the theoretical uncertainty from QED graph computations as well as the uncertainty from the strong interaction graphs (total $\approx \pm 10$ ppm) contribution has not been taken into account.

c) Here we have taken into account only the experimental errors: S.R. Lundeen and F.M. Pipkin, Phys. Rev. Letters 34, 1368 (1975). It has to be said that there is a rather big difference between the available theoretical calculations [see, G.W. Erickson, Phys. Rev. Letters 27, 780 (1971) and P.J. Mohr, Phys. Rev. Letters 34, 1050 (1975)] so that taking into account also this uncertainty, it would appear that in this case $\epsilon \approx 0.3\%$ (value in parentheses).

d) This lecture and Ref. 28.

e) This value is calculated taking into account also the r.m.s. charge radius uncertainty of helium.

f) See text (Fig. 7).

Figure captions

- Fig. 1 : a) Vacuum polarization potential of order $\alpha(\alpha Z)$ (Uehling's term).
b) Vacuum polarization potential of order $\alpha^2(\alpha Z)$ (Källén-Sabry term).
c) Vacuum polarization potential of order $\alpha(\alpha Z)^3$.
d) Lowest contribution in α to the "Lamb shift" (Bethe's term) \bar{l} lepton (μ or e).

Fig. 2 : Value of the function $\eta(r) = \alpha A + \alpha^2 B$ as function of r [see formula (2)]. a_{μ}^B, a_e^B are respectively the Bohr radius of the muonic atom $\mu^- P$ and the hydrogen atom: λ_{μ} and λ_e are respectively the reduced wavelength of the muon and the electron.

Fig. 3 : Schema of the lowest energy levels of the $(\mu\text{He})^+$ muonic ion.

Fig. 4 : Schematic view of the apparatus: M = CH₂ moderators; 1, 3, 4, 5 = plastic scintillators; 2 = anticoincidence Čerenkov counter (lucite); T = Invar steel vessel; V = useful muon-stopping volume; A₁, ..., A₈ = NaI(Tl) counters; DC = dye cell; DM = dielectric mirror (R = 30%); DG = diffraction grating (1200 lines/mm); SM = stepping motor driving DG; D1-D2 = photodiodes; C = internally gold-coated conical light pipe; W = antireflecting window; S = light beam splitters; TC = optical telescope.

Fig. 5 : The $2S_{1/2} - 2P_{3/2}$ resonance signal. Each datum point represents the number of events, normalized to the same number of stopped muons, per stepping motor position SMP; the scale in wavelength (shown below) is fixed by the calibration procedure (λ_1 and λ_2 are two lines of an Ar lamp, as specified in the text). The full-line curve drawn on the data is the result of a best fit analysis ($\chi^2 = 11$) with a Lorentzian line (assuming for Γ the theoretical value $\Gamma = 8 \text{ \AA}$) plus a constant background. For the central wavelength value of the Lorentzian line, we have obtained $\lambda_0 = 8116.8 \pm 1.5 \text{ \AA}$. Having Γ as a free parameter the best fit has given $\Gamma_{\text{exp}} = 7.2 \pm 2.8 \text{ \AA}$ and the same value for λ_0 . The theoretical prediction for λ_0 is 8118.0 ± 21.8 .

Fig. 6 : Experimental set-up for the experiment of Tauscher et al. (to be published, Ref. 29).

Fig. 7 : Comparison between the theoretical and experimental values for different lines as shown by the last analysis of Duhler et al. (to be published).

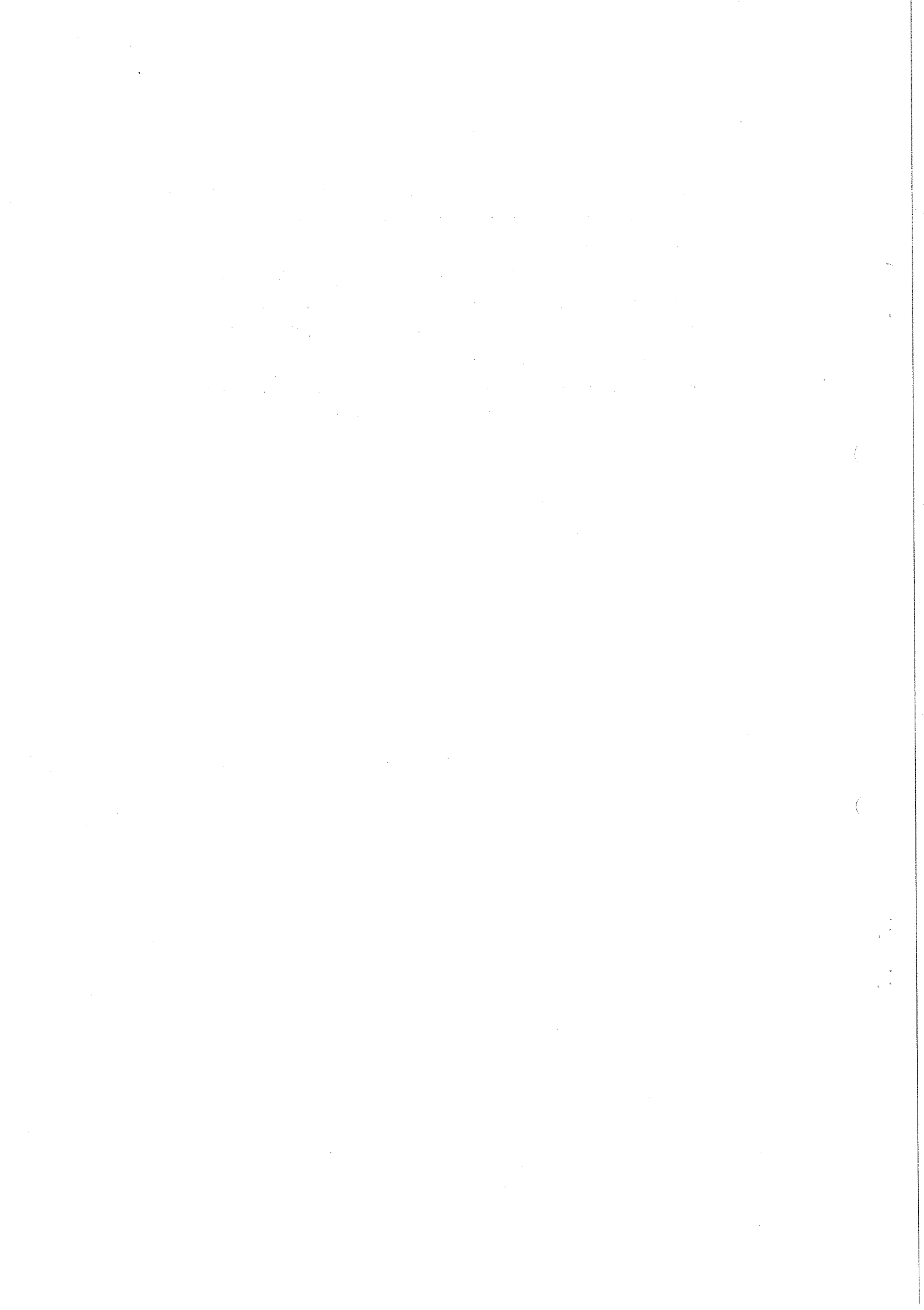
△ Tauscher et al., Phys. Rev. Letters 35, 410 (1975).

○ Dixit et al., Phys. Rev. Letters 35, 1633 (1975).

† Vuilleumier et al., Phys. Letters 40B, 197 (1972).

× Duhler et al., to be published.

● Theoretical estimates taken from the final analysis of Tauscher et al. (to be published, Ref. 29).



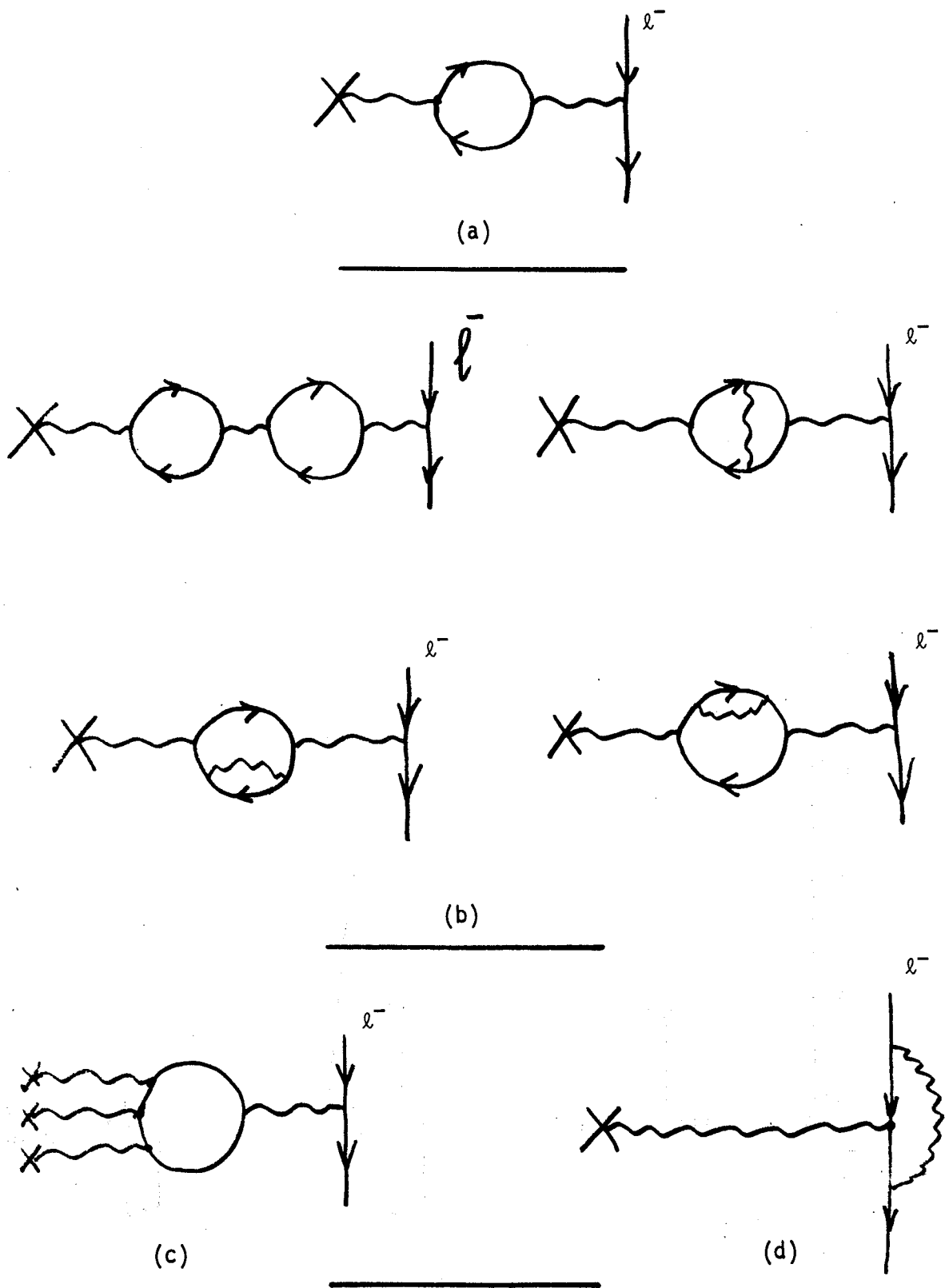


Fig. 1

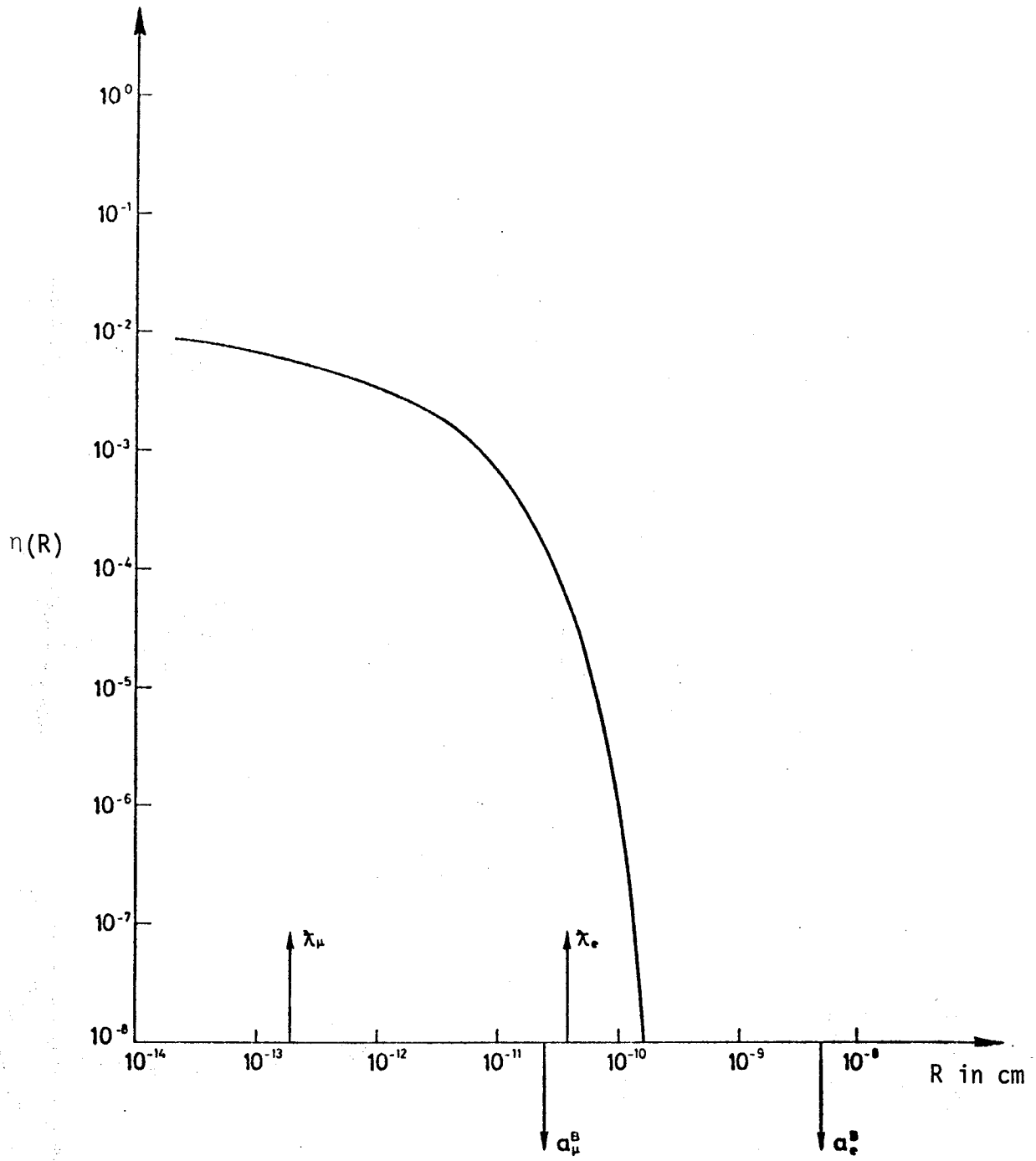


Fig. 2

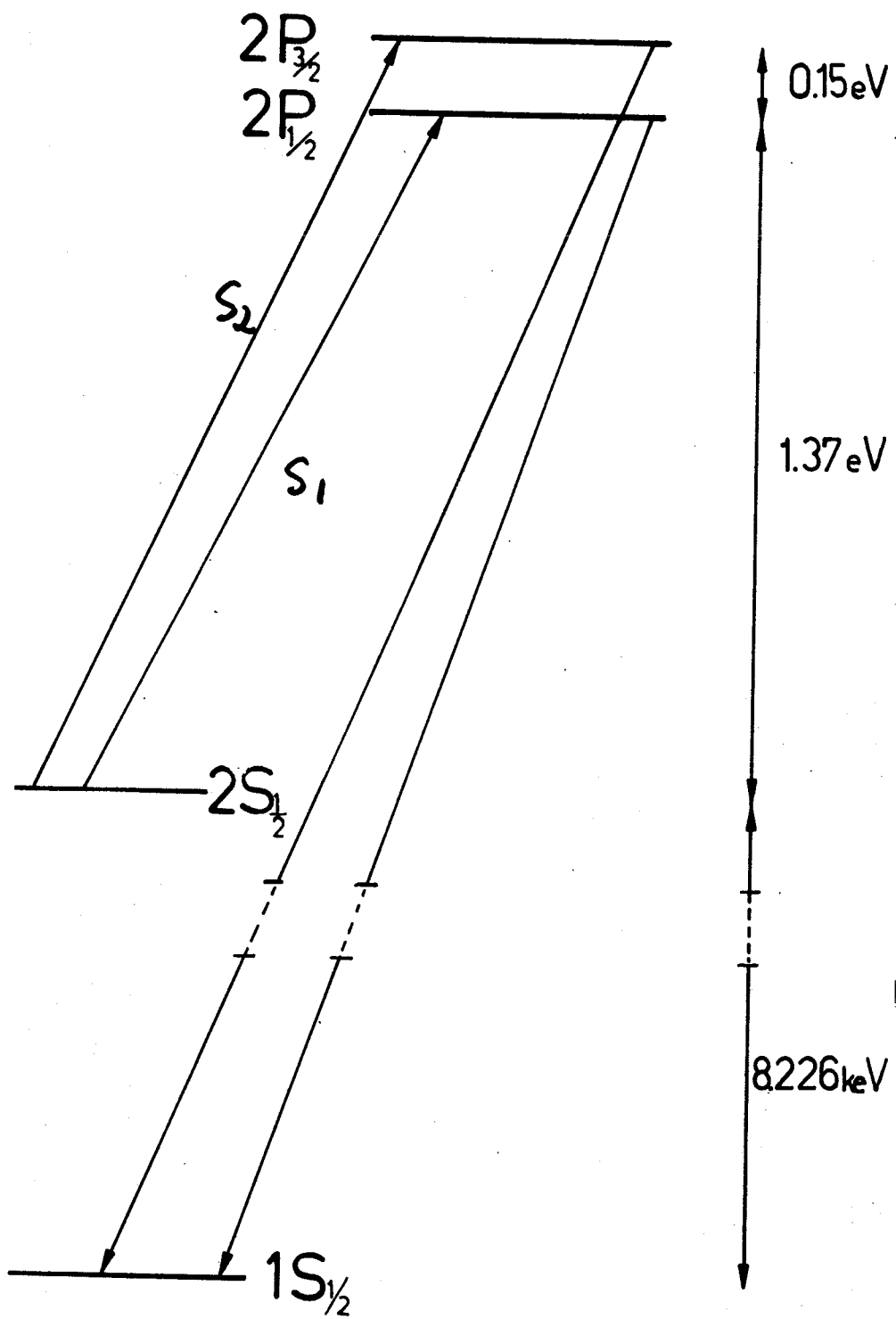


Fig. 3

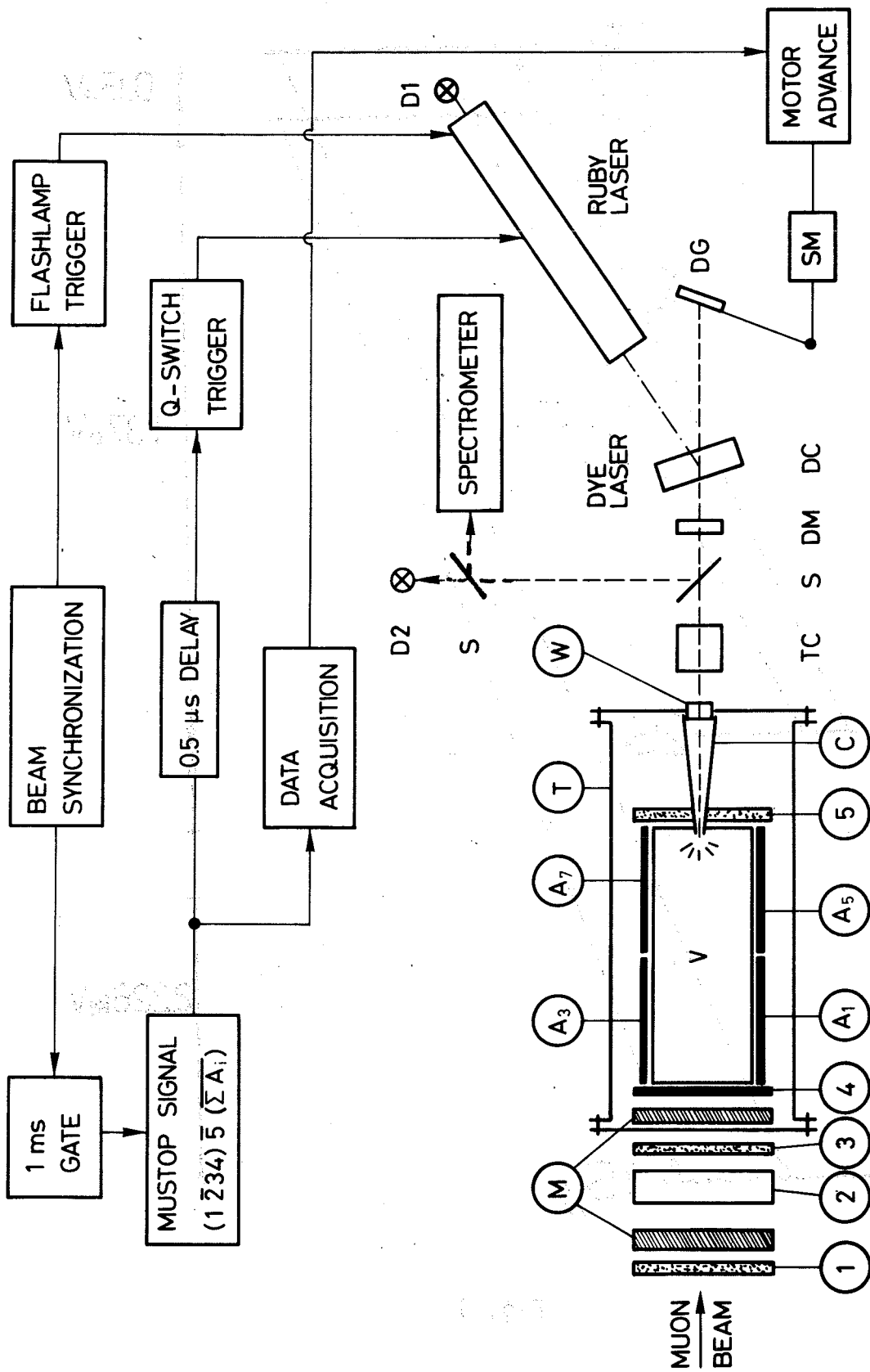


Fig. 4

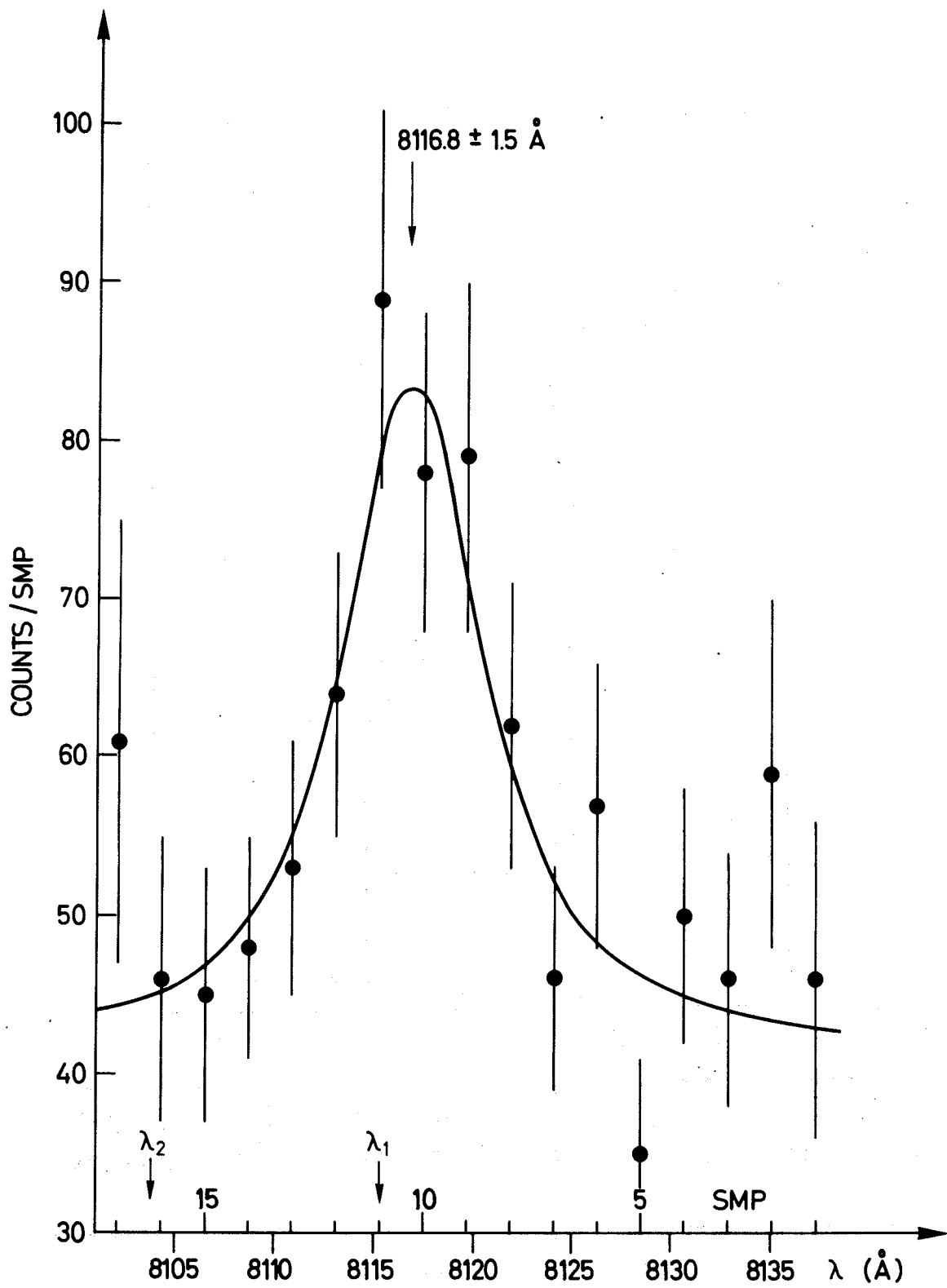
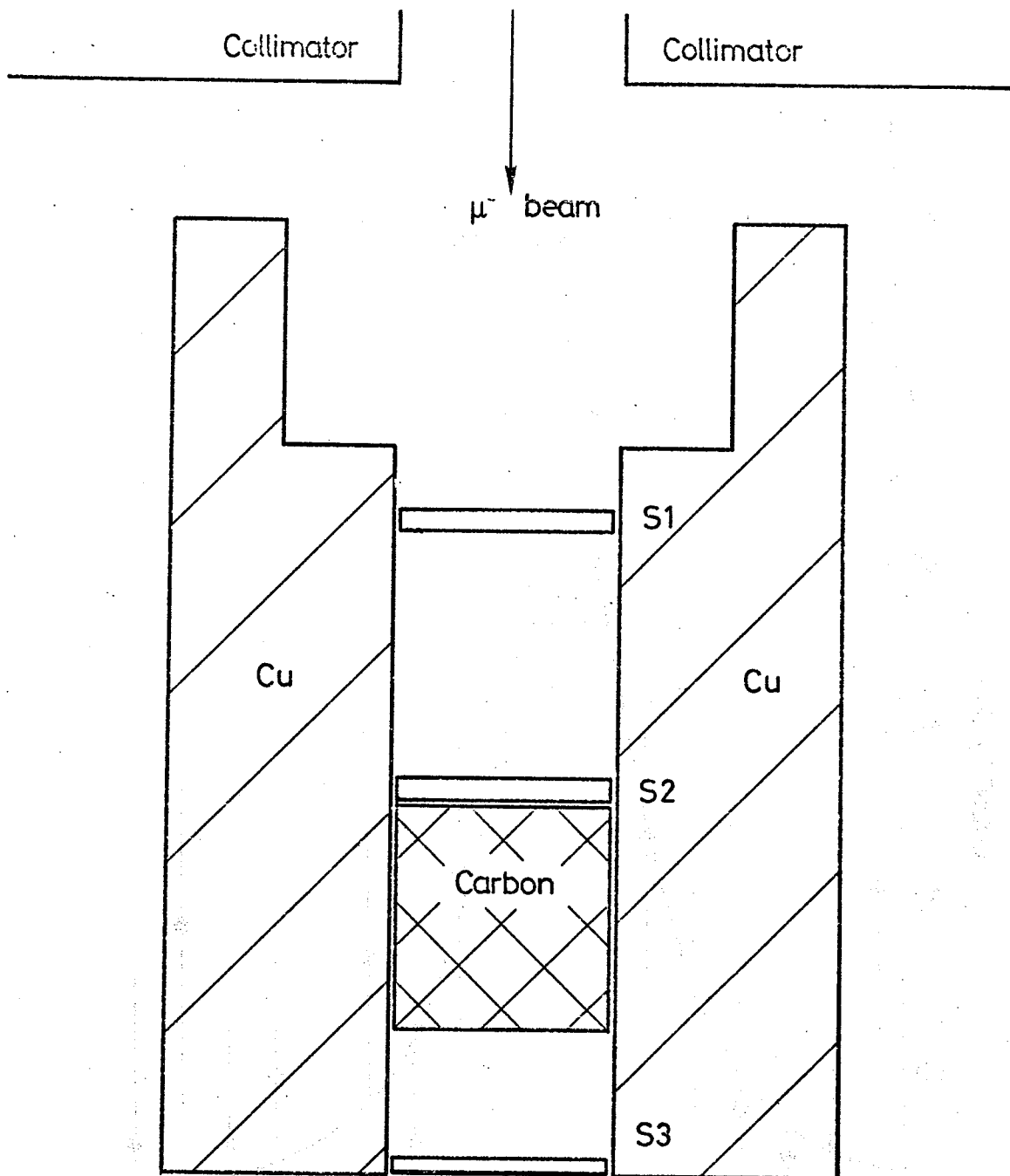
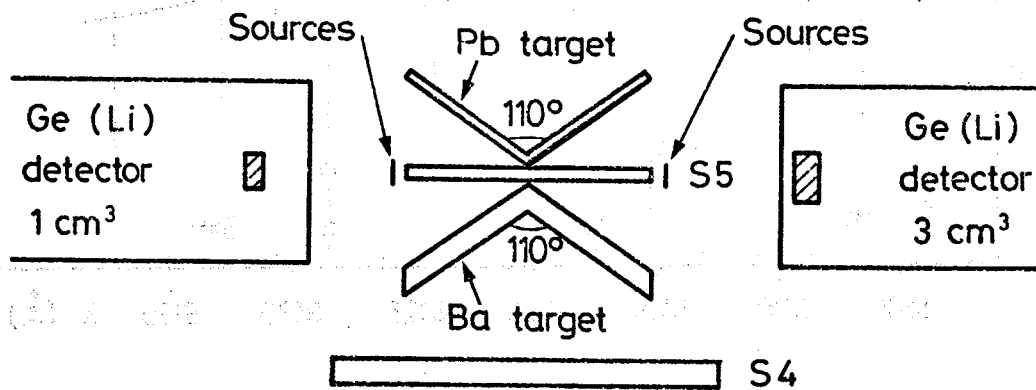


Fig. 5



65399



0 50 100 mm

Fig. 6

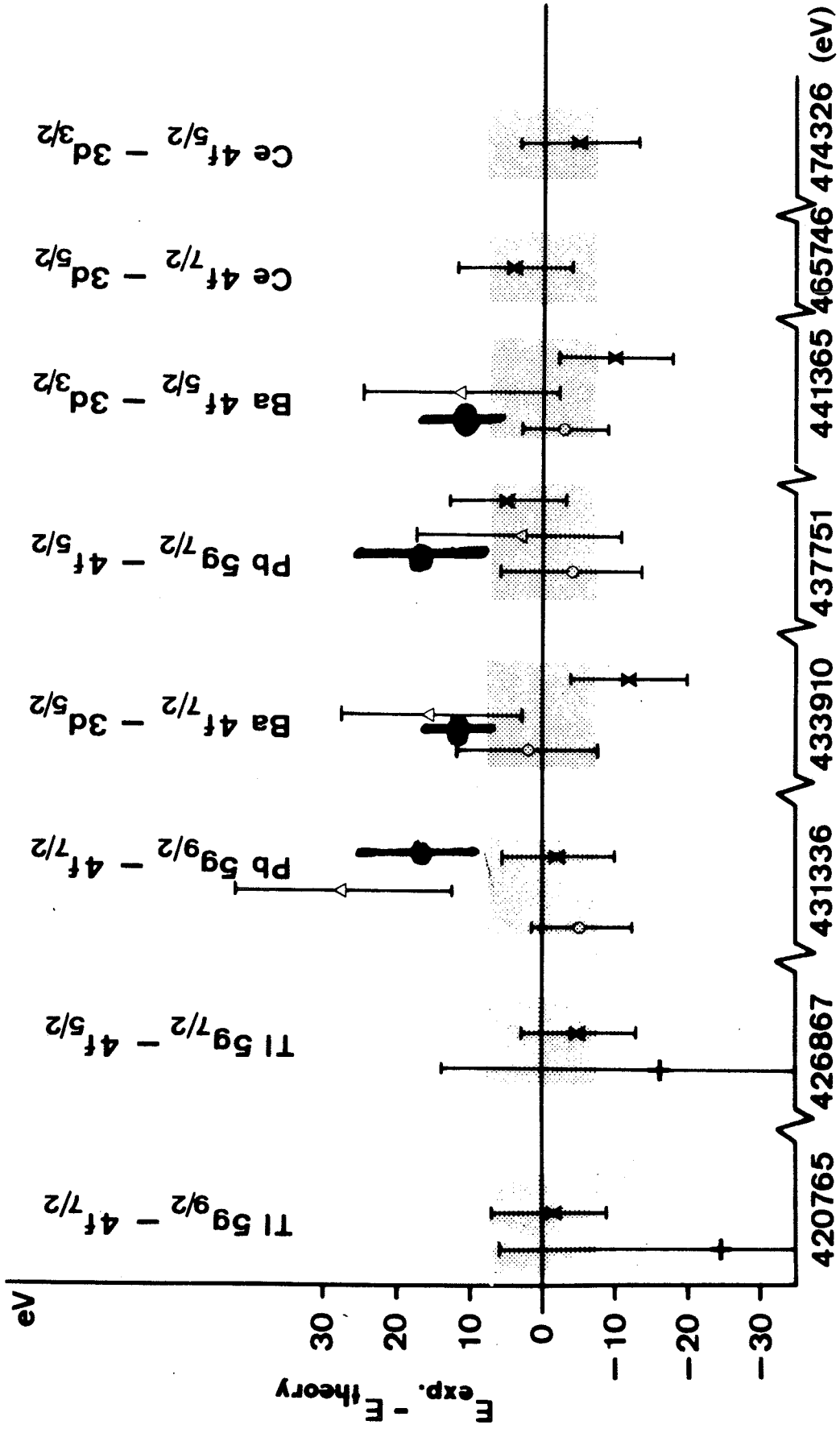


Fig. 7

